https://doi.org/10.15407/scine20.01.049
PYLYPENKO, O. V. (https://orcid.org/0000-0002-7583-4072),
DOLGOPOLOV, S. I. (https://orcid.org/0000-0002-0591-4106),
NIKOLAYEV, O. D. (https://orcid.org/0000-0003-0163-0891),
and KHORIAK, N. V. (https://orcid.org/0000-0002-4622-2376)
Institute of Technical Mechanics of the National Academy of Sciences
of Ukraine and State Space Agency of Ukraine,
15, Leshko-Popelya St., Dnipro, 49005, Ukraine,
+380 56 372 0640, +380 56 372 0640, office.itm@nas.gov.ua

MATHEMATICAL MODELING OF THE TRANSIENT PROCESSES IN PROPULSION SYSTEM OF THE UPPER STAGE OF THE CYCLONE-4M LAUNCH VEHICLE

Introduction. *The development of the Cyclone-4M space launch vehicle (LV) by Pivdenne Design Office is an important activity of the space industry of Ukraine. One of the LV innovations is feeding the liquid jet system (LJS) from the sustainer engine (SE) feedlines.*

Problem Statement. *In order to implement the specified method of the LJS feed, it is necessary to ensure the LJS operation during hydraulic shocks and pressure drops of the propellants during the SE start and shutdown. For this purpose, it is necessary to simulate the transient processes of the system start and shutdown.*

Purpose. *The purpose is to estimate the parameters of the transient processes of the Cyclone-4M upper stage sustainer engine, given the effect of SE on the LJS, as a result of their joint operation.*

Material and Methods. *The methods of the theory of automatic control, the impedance method, and the methods of numerical modeling of the unsteady motion of gas-saturated liquids have been used.*

Results. *The transient processes in the joint (SE and LJS) propulsion system during the start and shutdown have been simulated. In the developed mathematical model, we have used dynamic gains of feedlines as distributed and concentrated parameter systems, which are reconciled in a certain frequency range. The SE start and shutdown have been calculated. The experimental and the calculated values of natural frequencies of fluid oscillations, pressure peaks during hydraulic shocks, and the hydraulic shock patterns (horizontal pressure shelves when fluid continuity is broken) have shown a good agreement.*

Conclusions. *A nonlinear mathematical model of the low-frequency dynamics of the upper stage of propulsion system of the Cyclone-4M LV has been developed and tested. The model can be used to predict the time dependences of the propellant pressure at the LJS inlet during the SE start and shutdown in extreme conditions of LJS operation in the joint (the SE and the LJS) feed system.*

Keywords: the upper stage of the launch vehicle, liquid rocket engine and feed system, liquid jet system, transient processes, start and shutdown the engine, mathematical modeling.

Citation: Pylypenko, O. V., Dolgopolov, S. I., Nikolayev, O. D., and Khoriak, N. V. (2024). Mathematical Modeling of the Transient Processes in Propulsion System of the Upper Stage of the Cyclone-4M Launch Vehicle. *Sci. innov.*, 20(1), 49—67. https://doi.org/10.15407/scine20.01.049

The development of the *Cyclone-4M* space rocket complex by the State Enterprise Pivdenne Design Office in collaboration with *Pivdenmash*, other enterprises of the State Space Agency of Ukraine (SSAU), ITM of the National Academy of Sciences of Ukraine, alongside US and Canadian companies [1, 2], represents a pivotal direction in Ukraine's space industry. The innovation approach of powering the liquid jet system (LJS) of the upper stage of the *Cyclone-4M* launch vehicle from feedlines of the sustainer engine (SE) marks a global first in rocket and space system development. This innovation enables the elimination of an independent propellant feed system for the upper stage, enhances the upper stage's mass characteristics, and consequently, augments the payload capacity of spacecraft placed into operational orbits. However, this technical advancement presents a series of challenges [3] linked to the stability of the upper stage's motion control system during the start and stop of the RD861K sustainer engine's operation within the *Cyclone-4M* launch vehicle. The interconnected feed system of the SE and the LJS propagates hydraulic shocks and pressure fluctuations experienced during the sustainer engine's start and stop, transmitting them throughout the system without notable attenuation, eventually reaching the combustion chambers of the LJS. The reliability of the upper stage's thrust vector control for the *Cyclone-4M* rocket hinges upon the performance of the LJS under these extreme conditions.

It might be possible to study experimentally the LJS stability during the RD861K sustainer engine's start and stop, while making ground firing tests in the upper stage of the *Cyclone-4M* launch vehicle. However, these trials were carried out without activating the LJS combustion chambers because of inability to guarantee their operability under terrestrial conditions. The LJS combustion chambers functioned autonomously. To assess the upper stage's suitability for the flight conditions, there have been used the approach integrating mathematical modeling results of both the start and stop of the RD861K sustainer engine and the LJS performance under extreme hydraulic shocks and pressure fluctuations.

Studies [4, 5] have delved into the operation analysis of the control jet engines of the *Cyclone-4M* launch vehicle's upper stage during the start and stop sequences of the sustainer engine. The magnitude of pressure drops at the LJS inlet is established based on self-contained stage propellant feed system tests. However, the test conditions differ from the actual flight conditions, potentially leading to erroneous conclusions regarding LJS performance.

Addressing the challenge of determining transient processes in the propellant feed system of the launch vehicle's first stages during the activation of one or multiple engines has been outlined in [6—8]. The mathematical models developed in these studies describe low-frequency dynamic processes in the hydraulic and gas systems of the engine, accounting for fuel component transformation and residence delays in the gas generator, pump cavitation phenomena, and more. Research [9] has focused on defining the transient processes in the LPE propellant feed system during shutdown, investigating the effect of fluid pressure fluctuations and drops on the durability of in-tank devices.

The purpose of the research is to calculate the parameters of the transient processes in the feedlines of the sustainer engine of the multi-use upper stage of the *Cyclone-4M* launch rocket, given the influence of the sustainer engine on the operation of the LJS as a result of combining the feedlines into a single hydraulic system.

MATHEMATIC SIMULATION OF LOW-FREQUENCY DYNAMIC PROCESSES IN BRANCHED LINES OF LPE

The transient processes in liquid propulsion systems (LPS) occur during the start, stop, and transition of liquid propellant engines (LPE) to another mode of operation [10—13]. At the same time, hydraulic shocks usually occur during the filling of the pipelines when the front of the moving fluid ap-

proaches the pumps and local resistances, as well as when combustion starts in the gas generator and the combustion chamber of the engine. In case of the engine is stopped, hydraulic shocks appear when the compartment valves are closed.

The parameters of transient processes in the feedlines of the LPE during start and stop of the sustainer engine should be determined given the following phenomena and factors: energy dissipation in the fluid; acoustic phenomena in feedlines; the presence of free gas inclusions and the influence of the ductility of the walls of the pipelines on the speed of sound in the fluid; specific configuration of the feedline (branching, presence of concentrated elements, certain boundary conditions at the ends, etc.); the law of closing the valve. This approach involves the need for numerical mathematical simulation of transient processes in LPS during start and stop of the sustainer engine and usually includes the solution of the following problems [9]: mathematical simulation of the feedline as a distributed parameter system; approximation of the frequency characteristics of the feedline by finite hydrodynamic elements; numerical mathematical simulation of transient processes in LPS feedline during start and stop of the sustainer engine.

The LPE feedline usually has a complex branched network of pipelines with a large number of automation units for reliable engine start, smooth and sustainable operation, and stop. This especially applies to LPE of the upper stages of launch vehicle, for which the mass characteristics of the stage and the more compact arrangement of the LPE systems and aggregates are of primary importance.

It is expedient to consider LPE feedlines as distributed parameter systems. This makes it possible to take into account their length and branching, features of individual elements and boundary conditions with sufficient completeness and accuracy necessary for engineering calculations. The mathematical description of the fluid dynamics in the feedline sections is based on the equation of one-dimensional isothermal unsteady motion of the fluid and the equation of continuity [14, 15]:

$$\begin{cases} \dfrac{\partial p}{\partial z} + \dfrac{1}{g \cdot F} \cdot \dfrac{\partial G}{\partial t} + \dfrac{k}{g \cdot F} \cdot G = 0, \\ \dfrac{\partial G}{\partial z} + \dfrac{g \cdot F}{c^2} \cdot \dfrac{\partial p}{\partial t} = 0, \end{cases} \quad (1)$$

where p, G are the pressure and the mass flow of fluid; z is the coordinate of feedline axis; F is the area of the feedline cross section; k is the reduced coefficient of linear friction per unit length of the feedline; g is the acceleration of gravity; c is the speed of sound in the fluid flowing in a pipeline with elastic walls.

If the fluid contains undissolved gas, then the speed of sound in it is determined by the formula [10, 16]:

$$c = \frac{c_\infty}{\sqrt{1 + \dfrac{d \cdot E_L}{\delta \cdot E_S} + \dfrac{\varepsilon \cdot E_L}{p}}}, \; E_L = \frac{\lambda_L}{g} c_\infty^2, \quad (2)$$

where c_∞ is the speed of sound in the fluid in an unlimited volume; d and δ are the diameter and the thickness of feedline walls; E_S is the modulus of elasticity of the feedline wall material; ε is the volume fraction of undissolved gas; E_L is the modulus of elasticity of the fluid; γ_L is the specific gravity of the fluid.

To solve these equations in problems of the dynamics of pipeline systems, both the characteristic method [17] and the impedance method [18] have been used. The numerical method of characteristics is adapted for pipeline systems of different complexity, with different boundary conditions, it allows easily taking into account the presence of undissolved gases. The advantage of the impedance method is the ability to determine the spectrum of resonance frequencies of oscillations of a branched pipeline system. Also, with the use of the impedance solution method, a system of ordinary differential equations, which is combined with the system of differential equations, which describes the low-frequency dynamic processes in the engine, can be compiled to determine transient processes in the LPE feedlines.

To solve system of equations (1) by the impedance method [17] with respect to a homogeneous

section of the pipeline, a passive quadrupole may be composed as

$$\begin{cases} \delta\overline{p}_2 = b_{11}\cdot\delta\overline{p}_1 + b_{12}\cdot\delta\overline{G}_1, \\ \delta\overline{G}_2 = b_{21}\cdot\delta\overline{p}_1 + b_{22}\cdot\delta\overline{G}_1, \end{cases} \quad (3)$$

where $\delta\overline{p}_1$, $\delta\overline{G}_1$ are the deviation of the pressure and the fluid consumption at the inlet to the quadrupole from their values in the steady state; $\delta\overline{p}_2$, $\delta\overline{G}_2$ are the deviation of the pressure and the fluid consumption at the outlet from the quadrupole from their values in the steady state; b_{11}, b_{12}, b_{21}, and b_{22} are the elements of the transmission matrix of the pipeline section [17]:

$$b_{11} = ch(\gamma z),\ b_{12} = -sh(\gamma z)/Z_W,$$
$$b_{21} = -sh(\gamma z)Z_W,\ b_{22} = ch(\gamma z);$$

$\gamma = \sqrt{Z_1 Y_1}$ is the complex constant of wave propagation; $Z_W = \sqrt{Z_1/Y_1}$ is the wave resistance of the pipeline; $Z_1 = (j\omega + k)/gF$ is the serial hydraulic impedance of the pipeline; $Y_1 = j\omega\, gF/c^2$ is the parallel admittance of the pipeline; j is the imaginary unit; ω is the angular frequency of oscillations.

If there is given the boundary condition at the outlet from the pipeline section in the form of impedance $Z_2 = (j\omega)\dfrac{\delta\overline{p}_2(j\omega)}{\delta\overline{G}_2(j\omega)}$, from quadrupole equations (3), we may determine the impedance at the inlet to the feedline section $Z_1(j\omega)$ and the dynamic gain of the considered section of the feedline $W_1(j\omega)$:

$$Z_1(j\omega) = \frac{\delta\overline{p}_1(j\omega)}{\delta\overline{G}_1(j\omega)} = \frac{b_{12} - b_{22}\cdot Z_2(j\omega)}{b_{21}\cdot Z_2(j\omega) - b_{11}},$$

$$W_1(j\omega) = \frac{\delta\overline{p}_2(j\omega)}{\delta\overline{p}_1(j\omega)} = b_{11} + b_{12}\frac{1}{Z_1(j\omega)}.$$

Impedance at the inlet to each subsequent section of the pipeline $Z_i(j\omega)$ and the dynamic gain of fluid oscillations in each subsequent section of the pipeline $W_i(j\omega)$ are determined similarly. At the junction of three or more sections of the feedline, the frequency characteristics $Z_i(j\omega)$ and $W_i(j\omega)$ are determined from the conditions of the balance of flows in and out, and the equality of pressures in all branches of the feedline, which are joined. The frequency characteristics of the line: impedance $Z(j\omega)$ and amplification factor $W(j\omega)$ are determined by successive transfer of boundary conditions that are set in the form of impedance, through the entire feedline:

Based on the frequency characteristics $Z(j\omega)$ and $W(j\omega)$ we may define natural oscillation frequencies of the pipeline system, as well as its resistance to cavitation oscillations (if the system includes a cavitation pump) [17]. They can also be used to build and verify a mathematical model of a pipeline concentrated parameter system [11, 19].

When modeling non-stationary hydrodynamic processes in the LPS pipelines, the finite element method uses the simplest concentrated hydrodynamic elements: active resistance, mass and capacity, which are the primary cells of the finite elements. Each simplest element reflects one specific property of the modeled solid medium (viscosity, inertia, and compressibility, respectively) and is described by the equation of the corresponding fundamental physical law [11]. The extension lines are conventionally divided into sections that are different combinations of the simplest elements: hydraulic resistance a_i, inertial resistance J_i and compliance C_i. At the same time, the equations of motion and continuity take the following form:

$$\begin{cases} \dfrac{dG_i}{dt} = \left(p_i - p_{i+1} + a_i G_i^2\right)/J_i, \\ \dfrac{d\,p_i}{d\,t} = \left(G_i - G_{i+1}\right)\dfrac{1}{C_i} + r_i\left(\dfrac{d\,G_i}{d\,t} - \dfrac{d\,G_{i+1}}{d\,t}\right), \end{cases} \quad (4)$$

where r_i is the coupling coefficient that is usually taken as some part of the wave resistance c_i/F_i and used for coupling certain finite elements [11].

Coefficients a_i and J_i are determined by pressure drop Δp_i and fluid consumption G_i, as well as by the ratio of pipeline length l_i to pipeline cross section F_i:

$$a_i = \frac{\Delta p_i}{G_i^2},\ J_i = \frac{l_i}{g\,F_i}. \quad (5)$$

Concentrated compliances C_i in the first approximation are determined by the ratio of fluid-

volume in the section of pipeline V_i to the square of the speed of sound in fluid c_i:

$$C_i = \frac{g\,V_i}{c_i^2}. \qquad (6)$$

Further, the number and value of concentrated compliances are specified based on the required accuracy of matching in the specified frequency range of frequency characteristics $Z(j\omega)$ and $W(j\omega)$ of the pipeline as distributed parameter system and concentrated parameter system [19].

MATHEMATICAL SIMULATION OF LOW-FREQUENCY DYNAMIC PROCESSES IN THE FUEL FEED SYSTEM OF LPE RD861K

Figure 1 presents a simplified calculation scheme of the joint fuel feedline of the RD861K sustainer engine and LPS. According to the scheme, this feed system consists of a feedline to the sustainer engine, a refueling line, and a feedline to the LPS. At the start, stop, and in the established mode of operation of the engine, there is no fluid flow through the refueling line, this line is a dead end. However, it is not isolated from the general feed system, it is filled with fluid and contributes to the dynamics of the joint feedline.

With the use of the approach presented in the previous section to the mathematical simulation of transient processes in the feedlines of the LPE, the amplification coefficients of the feedline to the sustainer engine $W_{1F}(j\omega) = \delta\overline{p}_{1F} / \delta\overline{p}_{TF}(j\omega)$, the feedline to LPS $W_{DF}(j\omega) = \delta\overline{p}_{PF} / \delta\overline{p}_{DF}(j\omega)$, and the refueling line $W_{ZF}(j\omega) = \delta\overline{p}_{PF} / \delta\overline{p}_{ZF}(j\omega)$, which are considered to be distributed parameter systems have been determined. The dependence of their modules on the frequency of oscillations is shown in Fig. 2 curve 1. The figure features that the natural frequencies of the first mode of fluid oscillations in these lines have the following values: 27 Hz for the feedline to the sustainer engine, 15 Hz for the feedline to the LPS, and 19 Hz for the refueling line. These calculated frequency characteristics have been obtained given the presence of undissolved gas in the working fluid at volume fraction of undissolved gas ε = 0.04% and a gas cavity that has a volume of V_{GF} = 8 cm^3, in the bellows, which is located in the horizontal section of the fuel feedline to the sustainer engine.

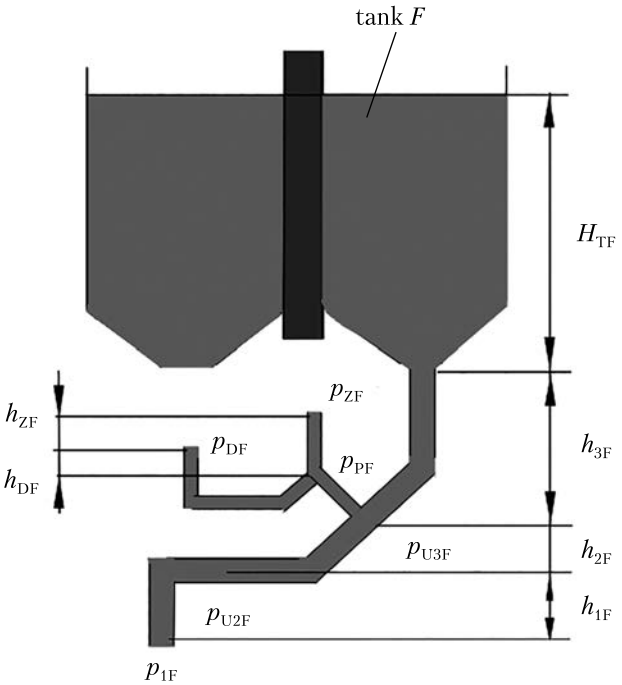

Fig. 1. Simplified calculation flowchart of the joint feedline of sustainer engine and LJS

For the transition from the distributed parameter system to the concentrated parameter system we have approximated the amplification coefficients of engine feedlines $W_{1F}(j\omega)$, $W_{DF}(j\omega)$, and $W_{ZF}(j\omega)$ with the help of hydrodynamic elements. When constructing the mathematical model of fluid dynamics in the feedline of the RD861K fuel engine as concentrated parameter system, we have assumed that the motion of fluid in the feedline to the RPS, as well as in the refueling line, is described by one oscillating link. The inertial resistance coefficient of the fluid in these two feedlines J_i is determined according to formula (5), while compliance coefficient C_i is calculated based on the frequency of oscillations of partial systems $\omega_i^2 = 1/(J_i C_i)$.

In the simulation, the fuel line to the sustainer engine is divided into three sections. In view of

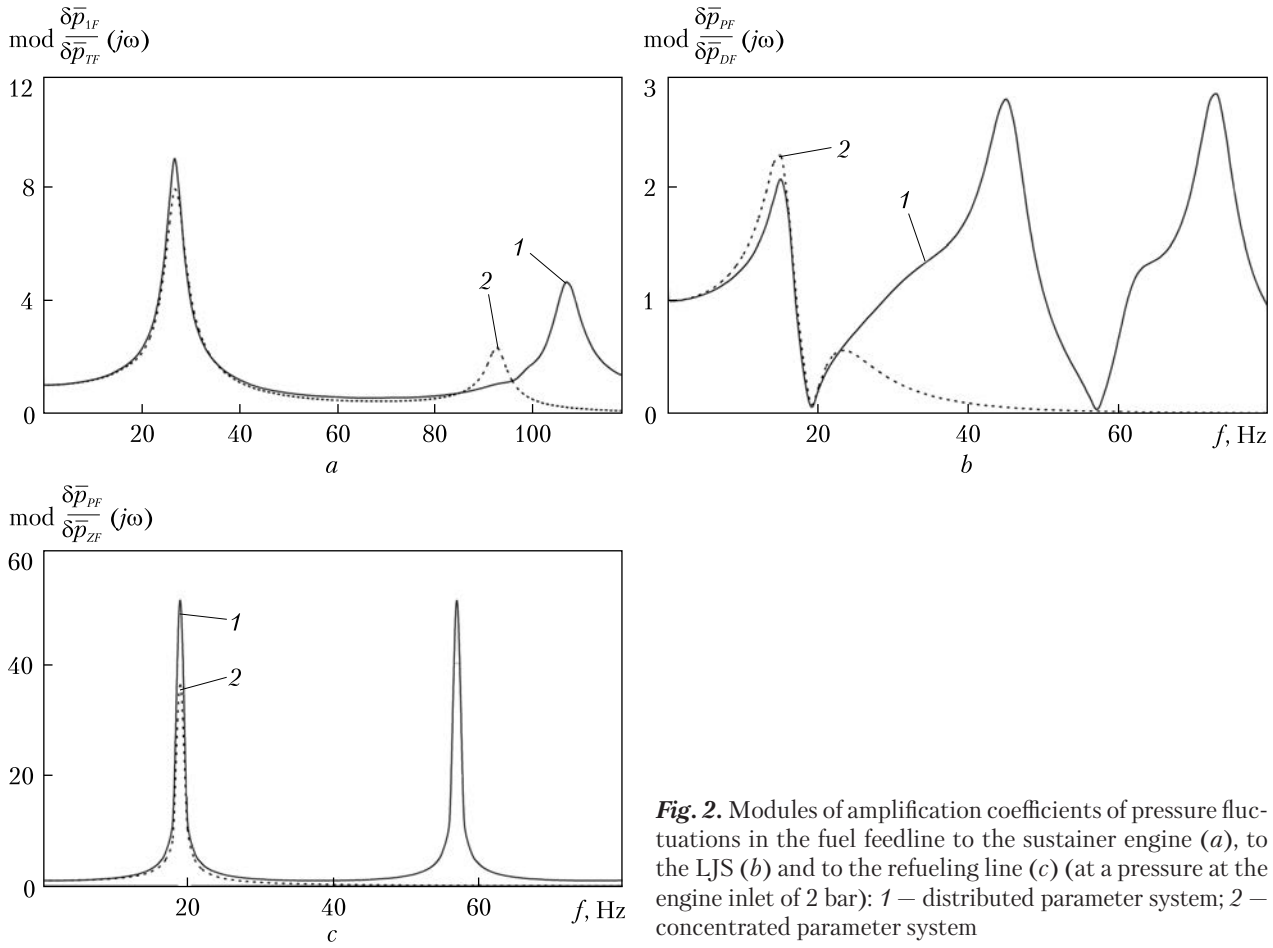

Fig. 2. Modules of amplification coefficients of pressure fluctuations in the fuel feedline to the sustainer engine (*a*), to the LJS (*b*) and to the refueling line (*c*) (at a pressure at the engine inlet of 2 bar): *1* — distributed parameter system; *2* — concentrated parameter system

the need to take into account its docking with the feedline to the RPS and the refueling line, as well as the presence of concentrated compliance in the bellows located in the horizontal section of the feedline, only the 1st tone of fluid fluctuations is taken into consideration. The compliance coefficients for the feedline to the sustainer engine have been determined in the first approximation by formula (6) and further refined by the amplification factor $W_{1F}(j\omega)$, as calculated for this feedline as distributed parameter system.

The coefficient of concentrated compliance in the bellows located in the horizontal section of the feedline for the sustainer engine has been determined by the formula [18]:

$$C_{U2F} = \frac{\gamma_F V_{GF}}{\kappa p_{U2F}}, \qquad (7)$$

where p_{U2F} is the fluid pressure in the place of bellows installation; γ_F is the fuel specific gravity; and κ is the adiabatic factor.

Figures 3 and 4 show the dependence of the compliance coefficients in the fuel line on the fluid pressure. We may see that the gas cavity in the bellows has the greatest compliance. Also, it should be noted that in the considered range of the fluid pressure variation, the compliance coefficients change approximately 5—45 times.

Figure 2 shows the modules of the amplification coefficients of the feedline to the sustainer engine $W_{1F}(j\omega)$, to the LPE $W_{DF}(j\omega)$ and the refueling line $W_{ZF}(j\omega)$, which are calculated based on mathematical simulation of dynamics of these feedlines as concentrated parameter systems (curve *2*). Their comparison with the previously ob-

tained amplification factors of the fuel feedline, as calculated on the basis of mathematical simulation of the dynamics of these lines as distributed parameter systems (curves *1*, Fig. 2) has shown their consistency for $W_{1F}(j\omega)$ within the frequency range up to 80 Hz, for $W_{DF}(j\omega)$ within the frequency range up to 25 Hz and for $W_{ZF}(j\omega)$ within the frequency range up to 40 Hz. Such frequency ranges are quite acceptable for describing the low-frequency dynamics of LPE feedlines.

For mathematical simulation of the transient processes directly in the feedlines during the start and stop of the RD861K sustainer engine, the mathematical model of the dynamics of these feedlines in concentrated parameters according to (4) has the form:

$$\overline{p}_{TF} = p_{U3F} + a_{U3F}G_{U3F}^2 + J_{U3F}\frac{dG_{U3F}}{dt} - (H_{TF} + h_{3F})\gamma_F, \quad (8)$$

$$G_{U3F}\frac{dp_{U3F}}{dt} = G_{U3F} - G_{U2F} - G_{PF} + r_{U3F}\left(\frac{dG_{U3F}}{dt} - \frac{dG_{U2F}}{dt} - \frac{dG_{PF}}{dt}\right), \quad (9)$$

$$p_{U3F} = p_{U2F} + a_{U2F}G_{U2F}^2 + J_{U2F}\frac{dG_{U2F}}{dt} - h_{2F}\gamma_F, \quad (10)$$

$$C_{U2F}\frac{dp_{U2F}}{dt} = G_{U2F} - G_{1F} + r_{U2F}\left(\frac{dG_{U2F}}{dt} - \frac{dG_{1F}}{dt}\right), \quad (11)$$

$$p_{U2F} = p_{1F} + a_{1F}G_{1F}^2 + J_{1F}\frac{dG_{1F}}{dt} - h_{1F}\gamma_F, \quad (12)$$

$$p_{U3F} = p_{PF} + a_{PF}G_{PF}^2 + J_{PF}\frac{dG_{PF}}{dt} - h_{PF}\gamma_F, \quad (13)$$

$$C_{PF}\frac{dp_{PF}}{dt} = G_{PF} - G_{DF} - G_{ZF} + r_{PF}\left(\frac{dG_{PF}}{dt} - \frac{dG_{DF}}{dt} - \frac{dG_{ZF}}{dt}\right), \quad (14)$$

$$p_{PF} = p_{DF} + a_{DF}G_{DF}^2 + J_{DF}\frac{dG_{DF}}{dt} - h_{DF}\gamma_F, \quad (15)$$

$$C_{DF}\frac{dp_{DF}}{dt} = G_{DF} - \overline{G}_{DF} + r_{DF}\frac{dG_{DF}}{dt}, \quad (16)$$

$$p_{PF} = p_{ZF} + a_{ZF}G_{ZF}^2 + J_{ZF}\frac{dG_{ZF}}{dt} - h_{ZF}\gamma_F, \quad (17)$$

$$C_{ZF}\frac{dp_{ZF}}{dt} = G_{ZF} - \overline{G}_{ZF} + r_{ZF}\frac{dG_{ZF}}{dt}, \quad (18)$$

where a_{U3F} a_{U2F}, a_{1F}, a_{PF}, a_{DF}, a_{ZF}, J_{U3F}, J_{U2F}, J_{1F}, J_{PF}, J_{DF}, and J_{ZF} are the hydraulic and inertial coefficients

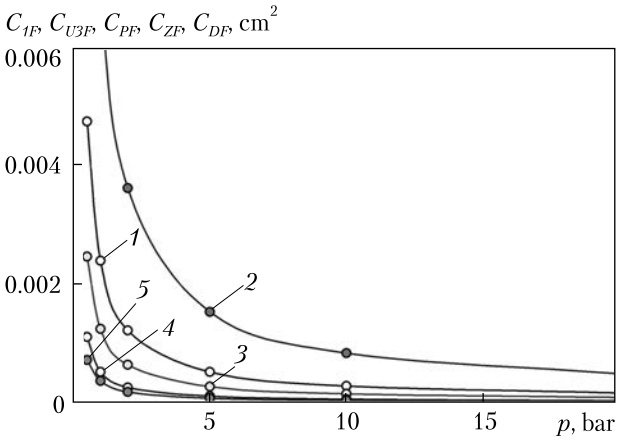

Fig. 3. Fluid pressure dependence of the compliance coefficients in the joint feedline of sustainer engine and LJS: *1* — C_{1F} at the engine inlet; *2* — C_{U3F} in the place of branching to the LJS and the refueling line; *3* — C_{PF} in the place of branching to the LJS and the refueling line; *4* — C_{ZF} in the refueling line; *5* — C_{DF} in the feedline to the LJS

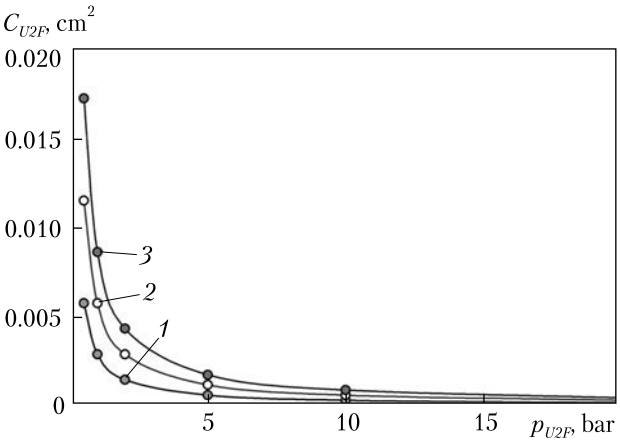

Fig. 4. Fluid pressure dependence of gas bulb compliance coefficient in the fuel feedline to the sustainer engine: *1* — at V_{GF} 4 cm^3; *2* — at V_{GF} 8 cm^3; *3* — at V_{GF} 12 cm^3

of the feedline respective sections; H_{TF}, h_{3F}, h_{2F}, h_{1F}, h_{PF}, h_{DF}, and h_{ZF} are the vertical projection of the respective fuel feedline sections; r_{U3F}, r_{U2F}, r_{PF}, r_{DF}, and r_{ZF} are the cost coupling coefficients of the respective sections of the fuel feedline; $\overline{G}_{DF}$ = const is feedline the boundary condition on the LJS; $\overline{G}_{ZF} = 0$ is the boundary condition on the fuel.

In the mathematical modeling of transient processes in the fuel feed system at the start of the

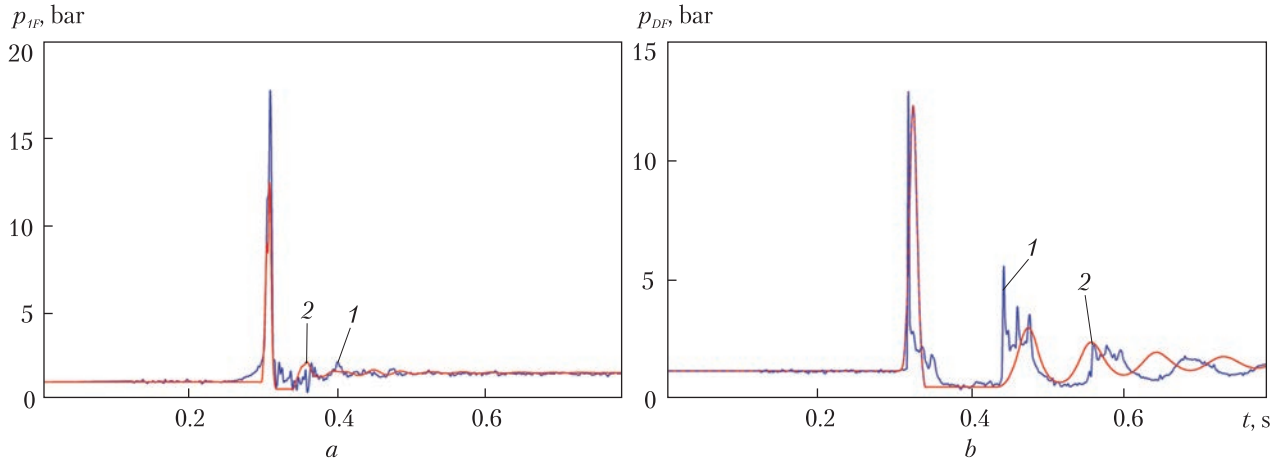

Fig. 5. Time dependence of fuel pressure at the engine inlet (*a*) and at the LJS inlet (*b*) during RD861K sustainer engine shutdown in the test conditions: *1* — experimentally measured; *2* — calculated

RD861K sustainer engine, the equation of the dynamics of cavities is used to determine the pressure at the engine inlet, which is presented below in the nonlinear model of the RD861K engine dynamics. While modeling the transient processes in the fuel feed system, when the engine is stopped, we use the following continuity equation:

$$G_{U1F}\frac{dp_{1F}}{dt} = G_{1F} - G_{MDF}(t), \qquad (19)$$

where $G_{MDF}(t)$ is the law of change in the fluid flow at closed shut-off valve at the inlet to the sustainer engine, which has been chosen experimentally:

$$G_{MDF}(t) = \overline{G}_{MDF}\left(1 - \frac{t}{t_{KF}}\right), \qquad (20)$$

where $\overline{G}_{MDF}$ is the stationary consumption through the sustainer engine; t_{KF} is the time of stopping the fluid feed through the shut-off valve.

It should be noted that this paper deals with, first of all, the transient processes in the joint feedline of the SE and the LJS and their effect on the performance of the LJS. When starting the SE and operating in a steady state, the dynamic processes in the engine affect the dynamics of the feedline. When stopped, the engine and its feedline are separated. The dynamic processes in the engine cannot affect the transient processes in the feedline and therefore they are not considered or modeled. Here, we focus our attention on the transient processes on the other side of the valve, exclusively in the engine feedline system.

To test the constructed nonlinear model of the dynamics of the fuel feedline of the RD861K engine (8)—(20), the transient processes in the fuel feedline have been calculated and compared with the dynamic tests that simulate engine shutdown.

Figure 5 presents the experimental and the calculated time dependences of fuel pressure at the engine inlet and at the LJS inlet when the RD861K SE is stopped in the test conditions. The analysis of the experimental data has shown that when the fuel shut-off valve is closed, a high-intensity hydraulic shock is realized in the trial line. The pressure near the shut-off valve in the feedline of the working fluid to the engine p_{1F} increases to 17.7 bar, while in the line that feeds the fluid to the LJS near the LJS inlet p_{DF} grows up to 13 bar. The presence of horizontal sections after the first pressure surge indicates a rupture of the fluid column both in the feedline to the engine and (to an even greater extent) in the feedline to the LJS. After the first intense oscillations (with the rupture of the fluid column), in the trial line, there is observed a rapidly decaying transient process with oscillations that have the shape close to harmonics and the frequencies close to the natural ones.

The results of calculations of hydraulic shock according to model (8)—(20) are given in Fig. 5. The analysis of these figures has shown a good agreement between the calculations and the experimental data obtained in the tests. In the calculations, there are horizontal pressure shelves that indicate the rupture of the fluid during hydraulic shock. The calculated natural frequencies of fluid oscillations in the feedlines to the sustainer engine and to the LJS are 28.5 Hz and 11.6 Hz, which is in good agreement with the experimental oscillation frequencies (23.8 Hz and 9.3 Hz), respectively.

The tests of nonlinear model (8)—(20) of the dynamics of the fuel feedline of the RD861K sustainer engine during the simulation of the engine shutdown have showed that this model allows calculating the pressure peaks during hydraulic shock, the natural frequencies of fluid oscillations, and the hydraulic shock patterns. Thus, this model can be recommended for the use in calculating the transient processes in the fuel feedlines, when the RD861K engine starts and stops under real conditions.

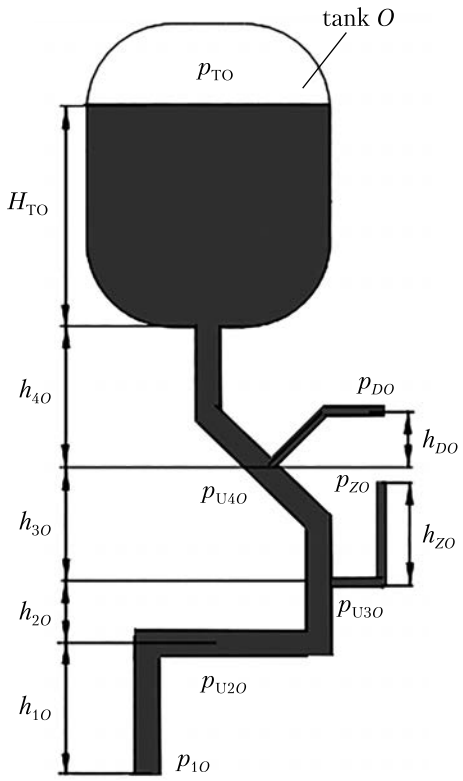

Fig. 6. Simplified calculation flowchart of the joint oxidant feedline of the sustainer engine and the LJS

MATHEMATICAL SIMULATION OF LOW-FREQUENCY DYNAMIC PROCESSES IN THE ROCKET ENGINE RD861K OXIDANT FEEDLINE

The low-frequency dynamic processes in the RD861K engine oxidant feedline have been simulated in a way similar to that used for the fuel feedline in the previous section. Therefore, it is briefly discussed in this section.

Figure 6 shows the design schematic of the RD861K engine oxidant feedline. It also consists of a feedline to the sustainer engine, a refueling line and a feedline to the LJS. With the use of feedlines, the amplification coefficients have been determined: for the oxidant feedline to the sustainer engine $W_{1O}(j\omega) = \delta\overline{p}_{1O} / \delta\overline{p}_{TO}(j\omega)$, for the feedline to the LJS $W_{DO}(j\omega) = \delta\overline{p}_{PO} / \delta\overline{p}_{DO}(j\omega)$, and for the refueling line $W_{ZO}(j\omega) = \delta\overline{p}_{PO} / \delta\overline{p}_{ZO}(j\omega)$, all considered as distributed parameter systems. Based on these frequency characteristics, the natural frequencies of the first mode of fluid oscillations in these lines have been determined: for the feedline to the sustainer engine (21.5 Hz), for the feedline to the LJS (45 Hz), and for the refueling line (38 Hz). These calculated oscillation frequencies have been obtained given the presence of undissolved gas in the working fluid at a volume fraction of undissolved gas $\varepsilon = 0.04\%$ and given the presence of gas cavity having a volume $V_{GO} = 10$ cm^3, which is located in the horizontal section of oxidant feedline to the sustainer engine, in the bellows.

In the mathematical modeling of the dynamics of the RD861K engine oxidant feedline as a concentrated parameter system, it is assumed that the dynamic processes in the feedline to the LJS and in the refueling line are described by one oscillating link. The feedline of the oxidant to the sustainer engine is conditionally divided into four

sections, with only the first mode of fluid fluctuations taken into consideration.

According to the calculation scheme of the joint oxidant feedline of the sustainer engine and LJS (see Fig. 6), a mathematical model of the dynamics of the oxidant feedline in concentrated parameters for the mathematical modeling of the transient processes has been developed:

$$\overline{p}_{TO} = p_{U4O} + a_{U4O}G_{U4O}^2 + J_{U4O}\frac{dG_{U4O}}{dt} - (H_{TO} + h_{4O})\gamma_O, \quad (21)$$

$$C_{U4O}\frac{dp_{U4O}}{dt} = G_{U4O} - G_{U3O} + G_{DO} + r_{U4O}\left(\frac{dG_{U4O}}{dt} - \frac{dG_{U3O}}{dt} + \frac{dG_{DO}}{dt}\right), \quad (22)$$

$$G_{DO}\frac{dp_{DO}}{dt} = G_{DO} - \overline{G}_{DO} + r_{DO}\frac{dG_{DO}}{dt}, \quad (23)$$

$$p_{DO} = p_{U4O} + a_{DO}G_{DO}^2 + J_{DO}\frac{dG_{DO}}{dt} - h_{DO}\gamma_O, \quad (24)$$

$$p_{U4O} = p_{U3O} + a_{U3O}G_{U3O}^2 + J_{U3O}\frac{dG_{U3O}}{dt} - h_{3O}\gamma_O, \quad (25)$$

$$C_{U3O}\frac{dp_{U3O}}{dt} = G_{U3O} - G_{U2O} + G_{ZO} + r_{U3O}\left(\frac{dG_{U3O}}{dt} - \frac{dG_{U2O}}{dt} + \frac{dG_{ZO}}{dt}\right), \quad (26)$$

$$G_{ZO}\frac{dp_{ZO}}{dt} = G_{ZO} - \overline{G}_{ZO} + r_{ZO}\frac{dG_{ZO}}{dt}, \quad (27)$$

$$p_{ZO} = p_{U3O} + a_{ZO}G_{ZO}^2 + J_{ZO}\frac{dG_{ZO}}{dt} - h_{ZO}\gamma_O, \quad (28)$$

$$p_{U3O} = p_{U2O} + a_{U2O}G_{U2O}^2 + J_{U2O}\frac{dG_{U2O}}{dt} - h_{2O}\gamma_O, \quad (29)$$

$$C_{U2O}\frac{dp_{U2O}}{dt} = G_{U2O} - G_{1O} + r_{U2O}\left(\frac{dG_{U2O}}{dt} - \frac{dG_{1O}}{dt}\right), \quad (30)$$

$$p_{U2O} = p_{1O} + a_{1O}G_{1O}^2 + J_{1O}\frac{dG_{1O}}{dt} - h_{1O}\gamma_O, \quad (31)$$

where a_{U4O}, a_{U3O}, a_{U2O}, a_{1O}, a_{DO}, a_{ZO}, J_{U4O}, J_{U3O}, J_{U2O}, J_{1O}, J_{DO}, and J_{ZO} are the hydraulic and inertial coefficients of the respective oxidant feedline sections; H_{TO}, h_{4O}, h_{3O}, h_{2O}, h_{1O}, h_{DO}, and h_{ZO} is the vertical projection of the respective sections of oxidant feedline; r_{U4O}, r_{U3O}, r_{U2O}, r_{DO}, r_{ZO} are the cost coupling coefficients in the respective sections of the oxidant feedline; γ_O is the share of oxidant; $\overline{G}_{DO}$ = const is the boundary conditions on the LJS; $\overline{G}_{ZO} = 0$ is the boundary condition on the refueling line.

In the mathematical modeling of the transient processes in the oxidant feedline at the start of the RD861K sustainer engine, we have used the equation of the dynamics of cavities to determine the pressure at the engine inlet, which is presented below in the nonlinear model of the RD861K engine dynamics. The following continuity equation has been used in the simulation of the transient processes in the oxidant feedline when the engine stops:

$$G_{U1O}\frac{dp_{1O}}{dt} = G_{1O} - G_{MDO}(t), \quad (32)$$

where $G_{MDO}(t)$ is the law of change in the fluid consumption when the shut-off valve at the sustainer engine inlet is closed, which has been chosen experimentally as

$$G_{MDO}(t) = \overline{G}_{MDO}\left(1 - \frac{t}{t_{KO}}\right), \quad (33)$$

where $\overline{G}_{MDO}$ is the stationary consumption of oxidant through the sustainer engine; t_{KO} is the time of stopping the feed of fluid through the shut-off valve.

To test the constructed nonlinear model of the dynamics of the RD861K oxidant feedline (21)–(33), the transient processes in the oxidant feedline have been calculated and compared with the dynamic tests that simulate engine shutdown.

Figure 7 presents the experimental and calculated time dependences of the oxidant pressure at the engine inlet and at the LJS inlet, when the RD861K MD stops in the test conditions. From the analysis of the experimental data, it follows that when the shut-off valve of the oxidant is closed, a high-intensity hydraulic shock occurs in the test pipeline. In the working fluid feedline to the sustainer engine, inlet pressure p_{1O} increases to 19.8 bar, while in the feedline to the LJS, near the LJS inlet, p_{DO} grows up to 23.8 bar. The presence of horizontal sections after the first pressure surge indicates a rupture of the fluid column in the entire feedline system. After the first intense oscillations (with the rupture of the fluid column), in the pipeline, there is observed a rapidly

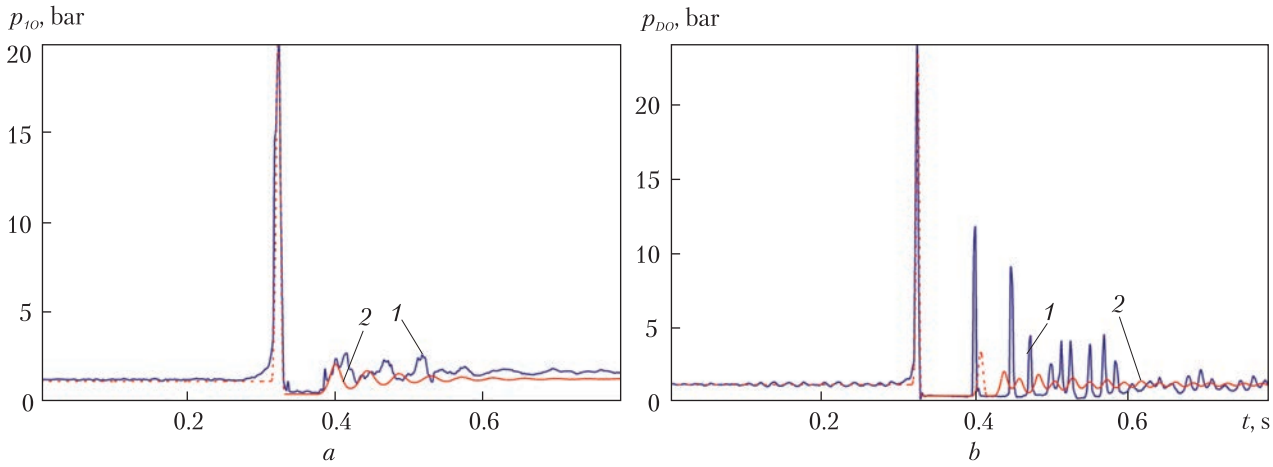

Fig. 7. Time dependence of oxidant pressure at the engine inlet (*a*) and at the LJS inlet (*b*) during RD861K sustainer engine shutdown in the test conditions: *1* — experimentally measured; *2* — calculated

decaying transient process with oscillations that have the shape close to harmonics and the frequencies close to the natural ones.

The results of calculations of hydraulic shock according to model (21)—(33) are given in Fig. 7. The analysis of these figures has shown a good agreement between the calculations and the experimental data obtained in the tests. In the calculations, there are horizontal pressure shelves that indicate the rupture of the fluid during hydraulic shock. The calculated natural frequencies of fluid oscillations in the feedlines to the sustainer engine and to the LJS are 22.7 Hz and 44.4 Hz, which is in good agreement with the experimental oscillation frequencies that range from 21 Hz to 27 Hz and from 45 Hz to 55 Hz, respectively.

The tests of nonlinear model (21)—(33) of the dynamics of the fuel feedline of the RD861K sustainer engine during the simulation of the engine shutdown have showed that this model allows obtaining the pressure peaks during hydraulic shock, the natural frequencies of fluid oscillations, and the hydraulic shock patterns, which are close to the experimental pressure peaks during hydraulic shock, the natural frequencies of fluid oscillations, and the hydraulic shock patterns (horizontal pressure shelves). Thus, this model can be recommended for the use in calculating the transient processes in the oxidant feedlines, when the RD861K engine starts and stops under real conditions.

MATHEMATICAL SIMULATION OF RD861K LPE START

Liquid propulsion single-chamber sustainer engine RD861K is designed according to the gas generator scheme. The main units and aggregates of the engine interact according to the pneumohydraulic scheme. The beginning of the engine start process is considered to be the moment of giving commands to open the inlet valves, when the engine paths begin to be filled with oxidant and fuel. The second command ensures the supply of helium to the starting nozzles of the turbine, with the turbopump (TP) rotor starting to rotate. Further, the oxidant and fuel valves on the gas generator get opened, with the cavities of the generator nozzle head starting to be filled with fuel components. Their ignition takes place in the fire space of the gas generator. The gas produced as a result of the combustion of fuel components enters the main turbine, with generator gas starting to spin-up the TP rotor. The oxidant and fuel flow into the combustion chamber cavities, and helium stops spinning up the TP rotor. Fur-

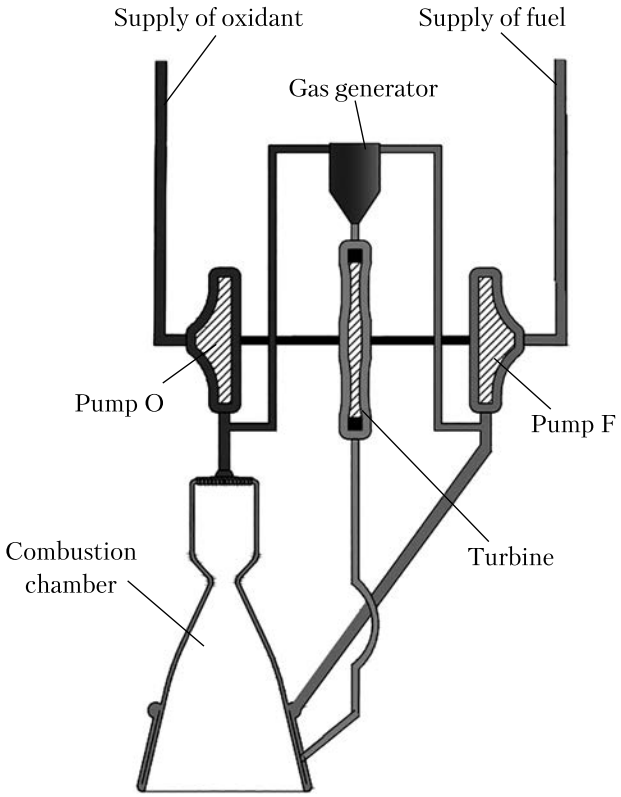

Fig. 8. Simplified calculation flowchart of RD861K sustainer engine

ther, the TP rotor is spun up by generator gas only. As the rotation frequency increases, the engine enters the main operation mode.

The mathematical model describing the nonlinear dynamics of the RD861K engine includes the mathematical models of the nonlinear dynamics of the joint oxidant and fuel feedline of the sustainer engine and the LJS (which have been presented and tested in the previous sections), as well as the mathematical model of the nonlinear dynamics of the RD861K engine itself. It should be taken into account that when solving many problems of the LPE dynamics and control, the units and aggregates of the engine in the low-frequency range (with frequencies up to 50 Hz) can be considered concentrated parameter systems, and their dynamics can be described by ordinary differential equations [14, 11]. The calculation scheme of the RD861K LPE (see Fig. 8) is based on its pneumohydraulic scheme and determines the composition of the mathematical model of the engine start. For the low-frequency range of processes reproduced during modeling, this model is a system of differential and algebraic equations and empirical ratios, which describe the change in the LPE parameters.

The start of the LPE in its initial period is usually accompanied by hydraulic shocks and pressure drops at the pumps inlets. This can cause cavitation failure of the pumps. In this regard, it is important to take into account the cavitation phenomena in the LPE pumps during the mathematical modeling of the LPE launch. Among the mathematical models of the dynamics of LPE cavitation pumps [18, 20—22], currently the most advanced group of mathematical models are those developed in the ITM of the NAS of Ukraine and SSAU [18, 20], which are based on the theory of jet cavitation flow around a grid of profiles and are called hydrodynamic models.

In this research, we have used a hydrodynamic model based on the generalization of the results of dynamic tests of 18 LPE screw centrifugal pumps and screw front pumps with a constant pitch [23]. It also uses the experimental and calculated coefficients obtained in [24—26]. This model contains the equation of the dynamics of cavities, which is written with respect to the pressure at the pump inlet, and the equation for determining the pressure at the pump outlet, like in [8]. With respect to the oxidant pump, these equations have the form:

$$(1+\alpha_{PO})\frac{dp_{1O}}{dt}=\frac{G_{1O}-G_{2O}}{C_{CO}}+R_{C1O}\frac{dG_{1O}}{dt}+R_{C2O}\frac{dG_{2O}}{dt}, \quad (34)$$

$$p_{UO}=p_{1O}+p_{PO}(\mathrm{n},G_{2O})\,\tilde{p}_{PO}-a_{2O}G_{2O}^2-$$
$$-(J_{2O}+J_{PO})\frac{dG_{2O}}{dt}, \quad (35)$$

where p_{1O}, G_{1O} are the fluid pressure and the consumption rate at the pump inlet; p_{UO}, G_{2O} are the fluid pressure and the consumption rate at the pump outlet; $\alpha PO=\frac{\partial(B_{1O}T_{CO})}{\partial p_{1O}}(G_{1O}-G_{2O})$ is the

ISSN 2409-9066. Sci. innov. 2024. 20(1)

dynamic coefficient; $C_{CO} = -\frac{\gamma_O}{B_{1O}}$ is the compliance of cavities in the oxidant pump; R_{C1O}, R_{C2O} are the cavitation resistance coefficients; B_{2O}: $R_{C1O} = B_{2O} - \frac{B_{1O} \cdot T_{CO}}{\gamma_O} + \frac{\partial p_{BD}}{\partial G_{1O}} - \frac{\partial (B_{1O} T_{CO})}{\partial G_{1O}} (G_{1O} - G_{2O})$; $R_{C2} = \frac{B_{1O} \cdot T_{CO}}{\gamma_O}$; $B_{2O}(p_{1O}, G_{1O}) = \frac{\partial p_{1O}}{\partial G_{1O}}$; B_{1O}, T_{CO} are the elasticity and the time constant of cavities; p_{BD} is the oxidant pump cut-off pressure; $p_{PO}(n, G_{2O})$, $\tilde{p}_{PO}$ are the pressure characteristic and the cavitation function of the oxidant pump; a_{2O},J_{2O} are the coefficients of hydraulic characteristics and the inertia of the oxidant feedline section from the pump outlet to the branch; J_{HO} is the inertia coefficient of the fluid in the flow part of the oxidant pump.

The mathematical model of the RD861K engine nonlinear dynamics along the oxidant line also contains the equations of the consumption rate balance in the branching of the pipelines and the equation of the oxidant motion from the pipeline branching to the fire space of the gas generator and the combustion chamber:

$$C_{UO} \frac{dp_{UO}}{dt} = G_{2O} - G_{CO} - G_{GGO}, \quad (36)$$

$$p_{UO} = p_C + a_{CO} G_{CO}^2 + J_{CO} \frac{dG_{CO}}{dt}, \quad (37)$$

$$p_{UO} = p_{GG} + a_{GGO} G_{GGO}^2 + J_{GGO} \frac{dG_{GGO}}{dt}, \quad (38)$$

where C_{UO} is the oxidant compliance coefficient in the pipeline branch; G_{CO}, G_{GGO} are the oxidant consumption rates for the combustion chamber and the gas generator; p_C, p_{GG} are the pressure in the combustion chamber and in the gas generator; a_{CO},J_{CO}, a_{GGO},J_{GGO} are the coefficients of hydraulic characteristics and the inertia of the oxidant feedline section from the branching of the pipelines to the combustion chamber and to the gas generator, respectively.

To make start calculations, the mathematical model of the RD861K engine nonlinear dynamics along the oxidant line shall be supplemented with the equations for filling the oxidant pipelines: from the oxidant inlet valve to the pipeline branching and from the pipeline branching to the fire space of the gas generator and to the combustion chamber:

$$\gamma_O \frac{dV_{PO}}{dt} = G_{2O}, \ \gamma_O \frac{dV_{CO}}{dt} = G_{CO}, \ \gamma_O \frac{dV_{GGO}}{dt} = G_{GGO} \quad (39)$$

where V_{PO}, V_{CO}, V_{GGO} are the filled volumes of the oxidant hydraulic paths from the oxidant inlet valve to the pipeline branching and from the pipeline branching to the fire space of the gas generator and the combustion chamber, respectively.

In the RD861K engine, the schemes of the oxidant and fuel hydraulic paths are similar (see the calculation scheme of the engine, Fig. 8): after the pumps, the flows of both fuel components are divided into the flow that go to the gas generator and the flow that comes to the combustion chamber. Therefore, the low-frequency dynamics of the fuel pump and its hydraulic path from the pump to the gas generator and the combustion chamber can be described by a system of equations similar to the one used to describe the low-frequency dynamics of the oxidant line (34)—(39).

When building the mathematical model of low-frequency dynamics of the RD861K LPE gas paths, the following generally accepted simplifications have been used [20, 27, 28]. The combustion chamber and the gas generator are considered concentrated parameter systems. The processes that take place in the gas paths of the engine are assumed to be adiabatic [20, 29]. No delays in the dynamics equations of the combustion chamber and the gas generator are taken into account. The simplifications make it possible to describe the non-stationary non-isothermal adiabatic motion of gas in the elements of engine's gas path within the frequency range up to 50 Hz with the hybrid system of equations, which consists of ordinary differential equations and algebraic equations. These equations are derived from the equations of continuity, conservation of momentum, conservation of energy, and the equation of state of gas. They describe changes in the pressure, the temperature, and the gas flow in the elements of the gas path

for the final cross-sections of each element (at the inlet and at the outlet).

Below, there are the equations that describe the working processes in the gas generator when the RD861K engine starts: for determining the pressure in the gas path of the gas generator, for determining the efficiency of fuel combustion products in the gas path of the gas generator, and for determining the consumption of combustion products at the gas generator outlet:

$$\frac{dp_{GG}}{dt} = \frac{\kappa_{GG}(RT)_{GG}}{V_{GG}}\left(G_{GGO} + G_{GGF} - G_{GG}\right), \quad (40)$$

$$(RT)_{GG} = (RT)(k_{GG}),\ k_{GG} = \frac{G_{GGO}}{G_{GGF}},$$

$$G_{GG} = \frac{F_{GG}\, p_{GG}}{\sqrt{(RT)_{GG}}}\sqrt{g\,\kappa_{GG}\left(\frac{2}{\kappa_{GG}+1}\right)^{\frac{\kappa_{GG}+1}{\kappa_{GG}-1}}}, \quad (41)$$

where $(RT)_{GG}$ is the performance of combustion products of fuel components in the gas generator; κ_{GG} is the adiabatic index in the gas generator; V_{GG} is the volume of the gas path of the gas generator; k_{GG} is the gas generator fuel component ratio; G_{GG} is the gas consumption through the gas generator; F_{GG} is the effective area of the nozzle grid of the engine turbine.

The working processes in the combustion chamber at the start of the RD861K engine are described by equations similar to (40) and (41).

For the mathematical modeling of the dynamics of the turbopump unit during the start of the RD861K LPE, as well as in stationary modes of operation of the engine, we have considered the motion of the rotor consisting of a shaft, impellers of turbines and pumps. The derivative of the angular momentum of the TP rotor relative to the fixed axis is equal to the momentum of the external forces applied to the rotor. Then the equations of the dynamics of the TP rotor and the torques of the turbines and the oxidant and fuel pumps on the TP shaft when starting the RD861K engine can be presented in the following form [27, 11]:

$$\frac{\pi}{30} J_{TPA} \frac{dn}{dt} = M_T + M_{TS} - M_{PO} - M_{PF}, \quad (42)$$

$$M_T = \frac{60}{2\pi\, n} G_{GG}\, L_{AD}\, \eta_T,$$

$$M_{TS} = \frac{60}{2\pi\, n} G_{TS}\, L_{ADS}\, \eta_{TS}, \quad (43)$$

$$M_{PO} = \frac{30}{\pi\, n} \frac{p_{PO}(n,\, G_{2O})G_{2O}}{\gamma_O\, \eta_{PO}},$$

$$M_{PF} = \frac{30}{\pi\, n} \frac{p_{PF}(n,\, G_{2F})G_{2F}}{\gamma_F\, \eta_{PF}} \quad (44)$$

where J_{TPA} is the moment of inertia of the TP rotor; M_T, M_{TS} are the torques of the LPE main and starting turbines; M_{PO}, M_{PF} are the torques of the oxidant and fuel pumps; $L_{AД}$ is the adiabatic work of the gas arriving at the blades of the main turbine

$$L_{AD} = \frac{\kappa_{GG}}{\kappa_{GG}-1}(RT)_{GG}\left(1 - \left(\frac{p_{T2}}{p_T}\right)^{\frac{\kappa_{GG}-1}{\kappa_{GG}}}\right), \quad (45)$$

p_T, pT_2 are the gas pressure at the inlet and outlet of the main turbine; η_T is the efficiency of the main TP turbine

$$\eta_T = \alpha_0 + \alpha_1\left(\frac{u}{c_{AD}}\right) + \alpha_2\left(\frac{u}{c_{AD}}\right)^2, \quad (46)$$

α_0, α_1, α_2 are the main TP turbine efficiency approximation coefficients; u is the peripheral speed of the turbine wheel on the average diameter; c_{AD} is the adiabatic gas velocity; L_{ADS} is the adiabatic work of the starting turbine gas; η_{TS} is the starting turbine efficiency; η_{PO}, η_{PF} are the efficiency of the oxidant and fuel pumps.

On the basis of the developed mathematical models of the fuel (8)—(18) and oxidant (21)—31) feedline system, as well as the model of the low-frequency dynamics of the RD861K sustainer engine (34)—(46), we have made calculations of the engine start. The main time characteristics of the engine start (the time dependence of pressure, consumption rate, and the frequency of TP shaft rotation) have been determined. The time required for oxidant and fuel to fill the tracts of the gas generator and combustion chamber has been estimated as 1.50 s and 1.99 s (gas genera-

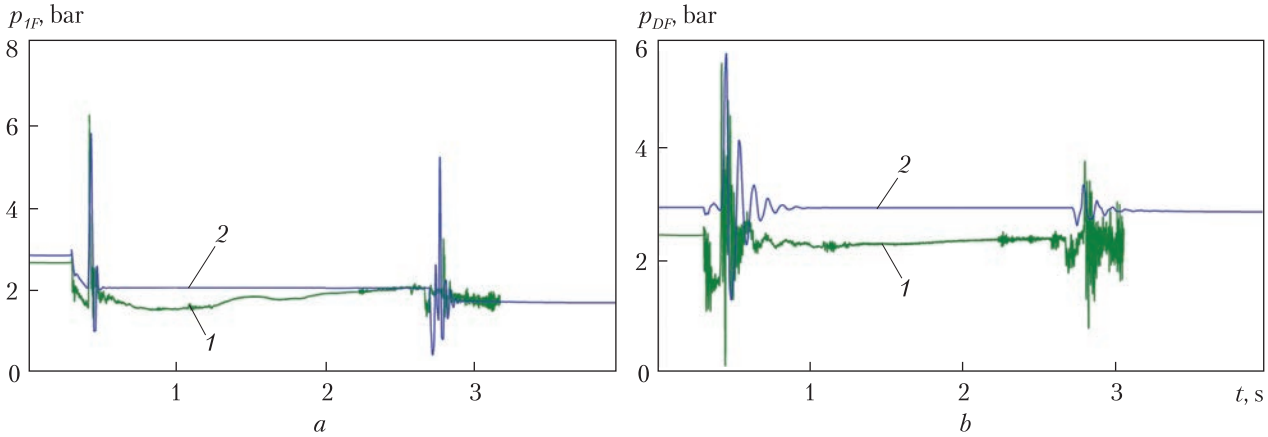

Fig. 9. Time dependence of fuel pressure at the engine inlet (*a*) and at the LJS inlet (*b*) during the start of RD861K sustainer engine in the test conditions: *1* — experimentally measured; *2* — calculated

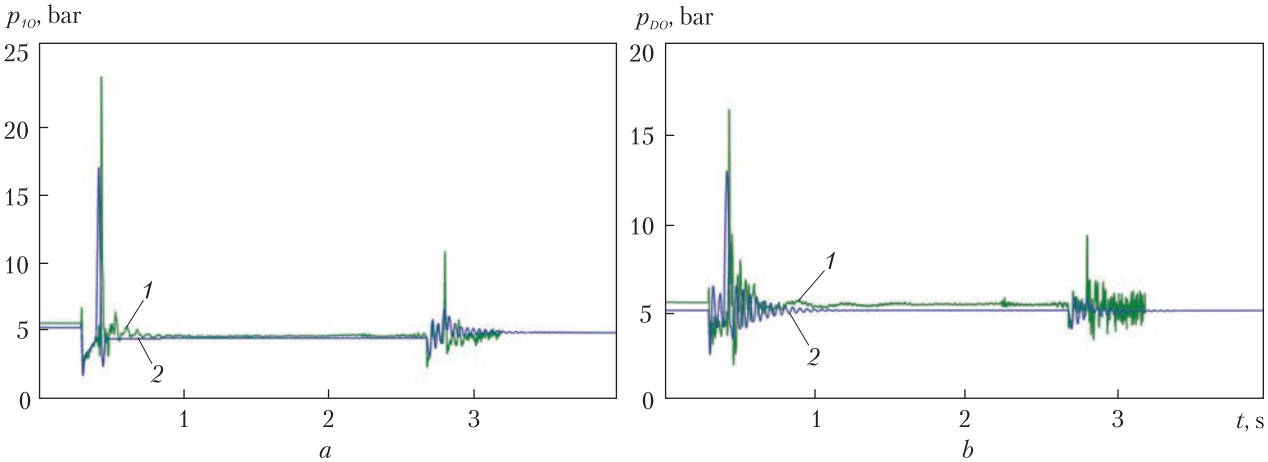

Fig. 10. Time dependence of oxidant pressure at the engine inlet (*a*) and at the LJS inlet (*b*) during the start of RD861K sustainer engine in the test conditions: *1* — experimentally measured; *2* — calculated

tor) and 2.37 s and 2.41 s (combustion chamber), respectively. The estimated time for the engine to enter the required mode (90% thrust) is 3.08 s. The time dependences of the transient process parameters in the joint system of the propulsion engine and LJS for both fuel components have been determined. For the pressure at the sustainer engine inlet and the LJS inlet, they are presented in Figs. 9 and 10 (here, the start time is conditionally assumed 0.3 s).

The same figures show the results of experimental studies. In general, the experimental and calculated data agree satisfactorily with each other. They have shown that during the engine start, there are two hydraulic shocks in the feedline system with both the oxidant and the fuel. During the first hydraulic shock, the pressure peaks occurs at a time of 0.44 s for the oxidant line and 0.42 s for the fuel line (in calculations, 0.42 s and 0.43 s, respectively). This hydraulic shock is caused by strong braking of the oxidant and fuel flows when they fill the pump impellers. At this start time, the TP shaft rotates slowly, which creates additional hydraulic pressure losses in the narrow channels of the pump impellers. The peak pressure at the sustainer engine inlet

during the first hydraulic shock is 23.6 bar, for the oxidant line, and 6.2 bar, for the fuel line (the calculated values are 17.0 bar and 5.8 bar, respectively). The peak pressure at the LJS inlet are slightly lower: 16.4 bar, for the oxidant line, and 5.5 bar, for the fuel line (the calculated values are 12.9 bar and 5.6 bar, respectively).

The second hydraulic shock is caused by braking the oxidant and fuel flows into the combustion chamber with a rapid increase in the pressure in the chamber due to ignition and subsequent combustion of fuel components. The pressure peaks during the second hydraulic shock occur at a time of 2.79 s (see Figs. 9 and 10). Their values are much smaller than those for the first hydraulic shock, and are at the sustainer engine inlet reach 10.4 bar, for the oxidant line, and 3.2 bar, for the fuel line (the calculated values are 6.7 bar and 5.2 bar, respectively), while at the LJS inlet they are equal to 9.4 bar, for the oxidant line and 3.7 bar , for the fuel line (the calculated values are 5.9 bar and 3.2 bar, respectively).

The nonlinear mathematical model of the low-frequency dynamics of the propulsion system of the upper stage of the *Cyclone-4M* launch rocket has been tested. It has been shown that the developed mathematical model makes it possible to satisfactorily describe the characteristics of transient processes during the start of a sustainer engine and to obtain the oxidant and fuel pressure peaks during hydraulic shocks, which are close to the experimental values. This means that the specified mathematical model can be used to predict the time dependence of the fuel component pressure at the LJS inlet during the start and stop of the sustainer engine, in extreme operating conditions of LJS in the joint feedline system of the sustainer engine and the LJS.

CONCLUSIONS

Nonlinear mathematical models of the low-frequency dynamics of the joint oxidant and fuel feedline systems of the sustainer engine and the upper stage of the *Cyclone-4M* launch vehicle have been developed. While developing them, we have used an approach that involves the determination and reconciliation of the frequency characteristics of fuel lines as distributed parameter systems and concentrated parameter systems, in a certain frequency range. The impedance method has been used to determine these frequency characteristics. The frequency characteristics of the feedlines have been calculated on the basis of the mathematical model of unsteady one-dimensional motion of a compressible fluid in a circular pipeline. For distributed parameter systems, these models are represented by partial differential equations. When considering the feedlines as concentrated parameter systems, we have used the simplest concentrated hydrodynamic elements such as active resistance, mass and capacity, which are the primary cells of finite elements, with the dynamics of feedlines described by ordinary differential equations.

To test the developed models, the transient processes in the oxidant and fuel feedlines during engine shutdown have been simulated. The comparison of the mathematical modeling results with the results of experimental studies has shown a satisfactory agreement of the pressure peaks during hydraulic shocks, natural frequencies of fluid oscillations, and hydraulic shock pattern (horizontal pressure shelves when fluid continuity is broken).

The mathematical model describing the nonlinear dynamics of sustainer engine has been developed. It contains the mathematical models of the nonlinear dynamics of the joint oxidant and fuel feedline of the sustainer engine and LJS and the mathematical model of the nonlinear dynamics of the RD861K engine itself. The engine model takes into account the cavitation phenomena in the oxidant and fuel pumps, the dynamics of filling the oxidant and fuel paths, gas-dynamic processes in the fire cavities of the gas generator and combustion chamber, and the dynamics of the TP rotor. The engine start parameters have been calculated. The main time characteristics of the engine start have been determined. The time required for oxidant and fuel to fill the tracts of the gas generator and combustion chamber and the time

for the engine to enter the required mode (90% thrust) have been estimated. It has been shown that during the engine start, there are two hydraulic shocks in the feedline system with both the oxidant and the fuel. The first hydraulic shock is caused by strong braking of the oxidant and fuel flows when they fill the pump impellers. The peak pressure at the sustainer engine inlet during the first hydraulic shock is 23.6 bar, for the oxidant line, and 6.2 bar, for the fuel line (the calculated values are 17.0 bar and 5.8 bar, respectively).

The second hydraulic shock is caused by braking the oxidant and fuel flows into the combustion chamber with a rapid increase in the pressure in the chamber due to ignition and subsequent combustion of fuel components. The pressure peaks are much smaller than those for the first hydraulic shock, and are at the sustainer engine inlet reach 10.4 bar, for the oxidant line, and 3.2 bar, for the fuel line (the calculated values are 6.7 bar and 5.2 bar, respectively).

The nonlinear mathematical model of the low-frequency dynamics of the propulsion system of the upper stage of the *Cyclone-4M* launch vehicle has been tested. It has been shown that the developed mathematical model makes it possible to satisfactorily describe the transient processes during the start and stop of a sustainer engine and can be used to predict the time dependence of the pressure at the LJS inlet during the start and stop of the sustainer engine, in extreme operating conditions of LJS in the joint feedline system of the sustainer engine and the LJS.

Funding. The research is funded within the framework of the innovation project approved by the Presidium of the National Academy of Sciences of Ukraine (Order No. 157 dated 07.03.2019) and under the contract II-27-19 dated April 1, 2019, between the NAS of Ukraine and the ITM of the NAS of Ukraine and SSAU (State Register number 0119U101216).

REFERENCES

1. National target scientific and technical space program of Ukraine for 2021—2025. http://materialy.kmu.gov.ua/af3b841c/docs/2b0a8327/Dodatok.pdf. (Last accessed: 25.04.2023) [in Ukrainian].
2. Space rocket systems. Launch vehicle Cyclone-4M. https://web.archive.org/web/20170727111416/http://yuzhnoye.com/ua/technique/launch-vehicles/rockets/cyclone-4m/ (Last accessed: 25.04.2023) [in Ukrainian].
3. Durachenko, V. M., Shpak, A. V., Kolesnichenko, S. A., Ageeva, L. I., Dolinkevich, A. S., Unchur, K. A. (2020). Problems and ways to solve them in the process of developing a liquid low-thrust jet engine for liquid rocket system of the 3rd stage of the Cyclone-4 launch vehicle. *Space Sci. & Technol.*, 26, 1(122), 18—29. https://doi.org/10.15407/knit2020.01.018 [in Russian].
4. Timoshenko, V. I., Knyshenko, Yu. V., Durachenko, V. M., Anishchenko, V. M. (2016). Issues of testing the control liquid propulsion system powered from the lines of the main engine of the last stage of the launch vehicle. *Space Sci. & Technol.*, 22(1), 20—35 [in Russian].
5. Timoshenko, V. I., Knishenko, Yu. V., Durachenko, V. M., Asmolovsky, S. Yu. (2020). Analysis of the robotic reactive engines of the upper stage of the Cyclone-4M launch vehicle during launches and stages of the main engine. *Technical mechanics*, 2, 22—35. https://doi.org/10.15407/itm2020.02.022 [in Russian].
6. Pylypenko, O. V., Prokopchuk, A. A., Dolgopolov, S. I., Pisarenko, V. Yu., Kovalenko, V. N., Nikolayev, O. D., Khoryak, N. V. (2017). Features of mathematical modeling of low-frequency dynamics of a sustainer staged liquid-propellant rocket engine at start-up. *Space Sci. & Technol.*, 23(5), 3—12. https://doi.org/10.15407/knit2017.05.003 [in Russian].
7. Pylypenko, O. V., Khoryak, N. V., Dolgopolov, S I., Nikolayev, O. D. (2019). Mathematical modeling of dynamic processes in hydraulic and gas paths at start-up of a staged liquid-propellant rocket engine. *Technical mechanics,* 4, 5—20. https://doi.org/10.15407/itm2019.04.005 [in Russian].
8. Pylypenko, O. V., Dolgopolov, S. I., Nikolayev, O. D., Khoryak, N. V. (2020). Mathematical modeling of the start-up of a multi-engine liquid rocket propulsion system. *Technical mechanics*, 1, 5—19. https://doi.org/10.15407/itm2020.01.005 [in Russian].

9. Dolgopolov, S. I., Zavoloka, A. N., Nikolayev, O. D., Sviridenko, N. F., Smolensky, D. E. (2015). Determination of the parameters of hydrodynamic processes in the propulsion system of the space stage during shutdowns and start-ups of the main engine. *Technical Mechanics*, 2, 23—36 [in Russian].
10. Belyaev, E. N., Chvanov, V. K., Chervakov, V. V. (1999). *Mathematical modeling of the working process of liquid-propellant rocket engines*. Moscow [in Russian].
11. Shevyakov, A. A., Kalnin, V. M., Naumenkova, M. V., Dyatlov, V. G. (1978). *Theory of Rocket Engine Automatic Control*. Moscow [in Russian].
12. Vasiliev, A. P., Kudryavtsev, V. M., Kuznetsov, V. A., Kurpatenkov, V. D., Obelnitsky, A. M., Polyaev, V. M., Poluyan, B. Ya. (1975). *Fundamentals of the theory and calculation of liquid rocket engines*. Moscow [in Russian].
13. Prisnyakov, V. F. (1983). *Dynamics of liquid-propellant rocket propulsion systems and power systems*. Moscow [in Russian].
14. Glikman, B. F. (1974). *Automatic control of liquid-propellant rocket engines*. Moscow [in Russian].
15. Charny, I. A. (1961). *Unsteady flow of real fluid in pipes*. Moscow [in Russian].
16. Glikman, B. F. (1979). *Unsteady flows in pneumohydraulic circuits*. Moscow [in Russian].
17 Fox, D. A. (1981). *Hydraulic analysis of unsteady flow in pipelines*. Moscow [in Russian].
18. Pilipenko, V. V., Zadontsev, V. A., Natanzon, M. S. (1977). *Cavitation oscillations and dynamics of hydraulic systems*. Moscow [in Russian].
19. Dolgopolov, S. I. (2006). Mathematical modeling of fluid dynamics in extended pipelines using hydrodynamic elements. *Technical mechanics*, 2, 114—120 [in Russian].
20. Pilipenko, V. V. (1989). *Cavitation self-oscillations*. Kyiv [in Russian].
21. Brennen, C. E., Meissner, C., Lo, E. Y., Hoffman, G. S. (1982). Scale effects in the dynamic transfer functions for cavitating inducers. *ASME J. Fluids Eng.*, 104, 428—433. https://doi.org/10.1115/1.3241875.
22. Brennen, C. E. (2012). A Review of the Dynamics of Cavitating Pumps (*IOP Conf. Ser.: Earth Environ. Sci. 15 012001 2012*). 1—13. https://doi.org/10.1088/1755-1315/15/1/012001.
23. Pilipenko, V. V., Dolgopolov, S. I. (1998). Experimental and computational determination of the coefficients of the equation for the dynamics of cavitation cavities in inducer centrifugal pumps of various sizes. *Technical mechanics*, 8, 50—56 [in Russian].
24. Dolgopolov, S. I. (1995). Generalized experimental-calculated coefficient of inertial resistance of a liquid caused by reverse flows at the inlet of a inducer-centrifugal pump. *Technical Mechanics*, 4, 99—103 [in Russian].
25. Dolgopolov, S. I. (2007). *Generalization of experimental stall pressures of cavitating inducer-centrifugal pumps of liquid propellant engines. Space technology. Missile weapons: 1*. Dnepropetrovsk [in Russian].
26. Pilipenko, V. V., Dolgopolov, S. I., Zadontsev, V. A., Grabovskaya, T. A. (2008). Experimental and computational method for determining the cavitation functions of pumps. Problems of high-temperature technology. Dnepropetrovsk [in Russian].
27. Alemasov, V. E., Dregalin, A. F., Tishin, A. P. (1980). *Theory of rocket engines*. Moscow [in Russian].
28. Natanzon, M. S. (1977). *Longitudinal self-oscillations of a liquid-propellant rocket*. Moscow [in Russian].
29. Glikman, B. F. (1989). *Automatic control of liquid rockets*. Moscow [in Russian].

Received 02.05.2023
Revised 16.06.2023
Accepted 20.06.2023

О.В. Пилипенко (https://orcid.org/0000-0002-7583-4072),
С.І. Долгополов (https://orcid.org/0000-0002-0591-4106),
О.Д. Ніколаєв (https://orcid.org/0000-0003-0163-0891),
Н.В. Хоряк (https://orcid.org/0000-0002-4622-2376)

Інститут технічної механіки Національної академії наук України
і Державного космічного агентства України,
вул. Лешко-Попеля, 15, Дніпро, 49005, Україна,
+380 56 372 0640, +380 56 372 0640, office.itm@nas.gov.ua

МАТЕМАТИЧНЕ МОДЕЛЮВАННЯ ПЕРЕХІДНИХ ПРОЦЕСІВ У СИСТЕМІ ЖИВЛЕННЯ МАРШОВОЇ РІДИННОЇ ДВИГУННОЇ УСТАНОВКИ ВЕРХНЬОГО СТУПЕНЯ РАКЕТИ-НОСІЯ «ЦИКЛОН-4М»

Вступ. Розробка ДП «КБ «Південне» космічної ракети-носія (РН) «Циклон-4М» є важливим напрямом роботи космічної галузі України. Одним з інноваційних способів живлення є живлення рідинної реактивної системи (РРС) з паливних магістралей маршового двигуна (МД).

Проблематика. Для реалізації зазначеного способу живлення РРС необхідно забезпечити стійкість роботи РРС при гідравлічних ударах та провалах тиску компонентів палива під час запуску й зупинки МД. Для цього виконують математичне моделювання перехідних процесів у маршовій двигунній установці при її запуску та зупинці.

Мета. Розрахункове визначення параметрів перехідних процесів у паливних магістралях маршового двигуна верхнього ступеня РН «Циклон-4М» з урахуванням впливу МД на роботу РРС внаслідок об'єднання магістралей їх живлення.

Матеріали й методи. Використано методи теорії автоматичного регулювання, імпедансний метод та методи чисельного моделювання неусталеного руху газонасичених рідин.

Результати. Проведено математичне моделювання перехідних процесів у спільній системі живлення МД та РРС верхнього ступеня РН «Циклон-4М» при запуску та зупинці МД. При розробці математичної моделі систем живлення двигунної установки були використані їхні частотні характеристики як систем із розподіленими та зосередженими параметрами, узгоджені у визначеному частотному діапазоні. Проведено розрахунки запуску та зупинки МД. Показано задовільне узгодження експериментальних та розрахункових значень власних частот коливань рідини, піків тиску при гідравлічних ударах і особливостей гідравлічного удару (горизонтальні полиці тиску при розриві суцільності рідини).

Висновки. Розроблено і протестовано нелінійну математичну модель низькочастотної динаміки двигунної установки верхнього ступеня РН «Циклон-4М», яку може бути використано для прогнозу залежностей тисків компонентів палива на вході в РРС від часу при запуску та зупинці МД, коли у спільній системі живлення МД та РРС реалізуються екстремальні для РРС режими роботи.

Ключові слова: верхній ступінь ракети-носія, маршовий рідинний ракетний двигун і його система живлення, рідинна реактивна система, перехідні процеси, запуск та зупинка двигуна, математичне моделювання.